Calix[4]arene Amino Acid Derivatives. Intra- and Intermolecular Hydrogen-Bonded Organisation in Solution and the Solid State

Leo Frkanec,[a] Aleksandar Višnjevac,[b] Biserka Kojić-Prodić,[b] and Mladen Žinić*[a]

Abstract: Chiral calix[4]arene derivatives with four *O*-(*N*-acetyl-PhgOMe), (**1**), (Phg denotes *R*-phenylglycine), or *O*-(*N*-acetyl-LeuOMe) (**2**) strands have been synthesised. Both compounds exist in chloroform in stable *cone* conformations with a noncovalently organised cavity at the lower rim that is formed by circular interstrand amidic hydrogen bonds. Such organisation affects both the selectivity and extraction/transport properties of **1** and **2** toward metal cations. Calix[4]arene derivatives with one $OCH_2COPhgOMe$ strand (**3**), two $OCH_2COPhgOMe$ strands (**5**) and with 1,3-OMe-2,4-($O-CH_2COPhgOMe$) substituents (**4**) at the lower rim have also been prepared. For **3**, a conformation stabilised by a circular hydrogen-bond arrangement is found in chloroform, while **4** exists as a time-averaged C_2 conformation with two intramolecular $NH\cdots OCH_3$ hydrogen bonds. Compound **5** has a unique hydrogen-bonding motif in solution and in the solid state with two three-centred $NH\cdots O$ and two $OH\cdots O$ hydrogen bonds at the lower rim. This motif keeps **5** in the flattened *cone* conformation in chloroform. The X-ray structure analysis of **1** revealed a molecular structure with C_2 symmetry; this structure is organised in infinite chains by intra- and intermolecular H bonds. The solid-state and solution structures of the [**1**-Na]ClO_4 complex are identical, C_4 symmetric *cone* conformations.

Keywords: calixarenes · cations · hydrogen bonds · noncovalent interactions · structure elucidation · supramolecular chemistry

Introduction

In biological systems, the cooperative action of peptidic hydrogen bonds plays a major role in organisation, assembly and molecular recognition processes.[1] The supramolecular approach to synthetic molecules with recognition and self-organisational properties often comprises synthetic combination of rigid molecular scaffolds that act as topological templates with amino acids or small peptides as organisational elements; various constrained systems such as cavitands,[2] steroids,[3] porphyrins,[4] constrained peptides[5] and sugars[6] have been used. Surprisingly, calix[4]arenes,[7] although they have been very extensively studied in recent years, have only been used infrequently as topological templates in combination with amino acids or peptides.[8] Very recently, however, the syntheses of calix[4]arene hybrid receptors functionalised at the upper rim with L-alanine and dipeptide units have been reported.[9] Very limited data are available in the literature about the upper-[8c, 9] or lower rim[8a, b] calix[4]arene tetra-(*O*-amino acid or -dipeptide) derivatives that describe their organisation by intramolecular hydrogen bonds. For structurally related cavitands[2] with strands at the lower rim that incorporate peptidic functionalities, organisation by intra- and interstrand hydrogen bonding was observed. However, the calix[4]arenes with urea units at the upper rim form dimers through intermolecular hydrogen bonds and produce a molecular capsule.[10, 11] An example of the lower rim 1,3-bis-*O*-(CH_2CONHR)-substituted calix[4]arene revealed the transannular amidic type of hydrogen bonding.[12] All of the above examples show that calix[4]arene derivatives with hydrogen-bonding functionalities at the lower or upper rim may form various types of intra- or intermolecular organisations.

The possible hydrogen-bonding motifs of calix[4]arene derivatives with one, two or four strands at the lower rim and with one amino acid unit each are presented in this work. Molecular modelling studies[13] on *p-tert*-butyl-calix[4]arene (**1**, Scheme 1) in the *cone* conformation with four *O*-($CH_2COPhgOMe$) strands at the lower rim show that the interstrand peptidic type of hydrogen bonding is likely to occur with this type of calix[4]arene. More interestingly, if all

[a] Prof. M. Žinić, L. Frkanec
Laboratory for Supramolecular and Nucleoside Chemistry
Rudjer Bošković Institute, P.O. Box 1016
10001 Zagreb (Croatia)
Fax: (+385) 1-46-80-195
E-mail: zinic@rudjer.irb.hr

[b] A. Višnjevac, Dr. B. Kojić-Prodić
Laboratory for Chemical Crystallography and Biocrystallography
Rudjer Bošković Institute, P.O. Box 1016
10001 Zagreb (Croatia)

Supporting information for this article is available on the WWW under http://www.wiley-vch.de/home/chemistry/ or from the author.

0947-6539/00/0603-0442 $ 17.50+.50/0 *Chem. Eur. J.* **2000**, *6*, No. 3

the amide groups are oriented in the same direction, the hydrogen bonds may form a circular arrangement and this offers additional benefits of cooperativity. Such compounds appear to be of interest with respect to the known metal cation binding properties of calix[4]arene tetra-(*O*-acetamide) derivatives.[14] In order to investigate experimentally the anticipated organisational properties of such calix[4]arene amino acid derivatives, we have synthesised the tetrasubstituted calix[4]arene derivatives **1** and **2**. In addition, mono- (**3**) and disubstituted derivatives (**4** and **5**) have been prepared to investigate possible hydrogen-bonding motifs with OH and amidic functions at the lower rim (Scheme 1). The acyclic model compound **6** was prepared for comparative purposes. The solution and solid-state structures of prepared calixarenes were studied by NMR and FTIR spectroscopy, and X-ray structure analysis. Metal cation extraction and transport studies were performed and the results were compared with those for calix[4]arene tetra-(*O*-acetamide) derivatives to reveal the possible dependence of these properties on hydrogen-bonding motifs present at the lower rim.

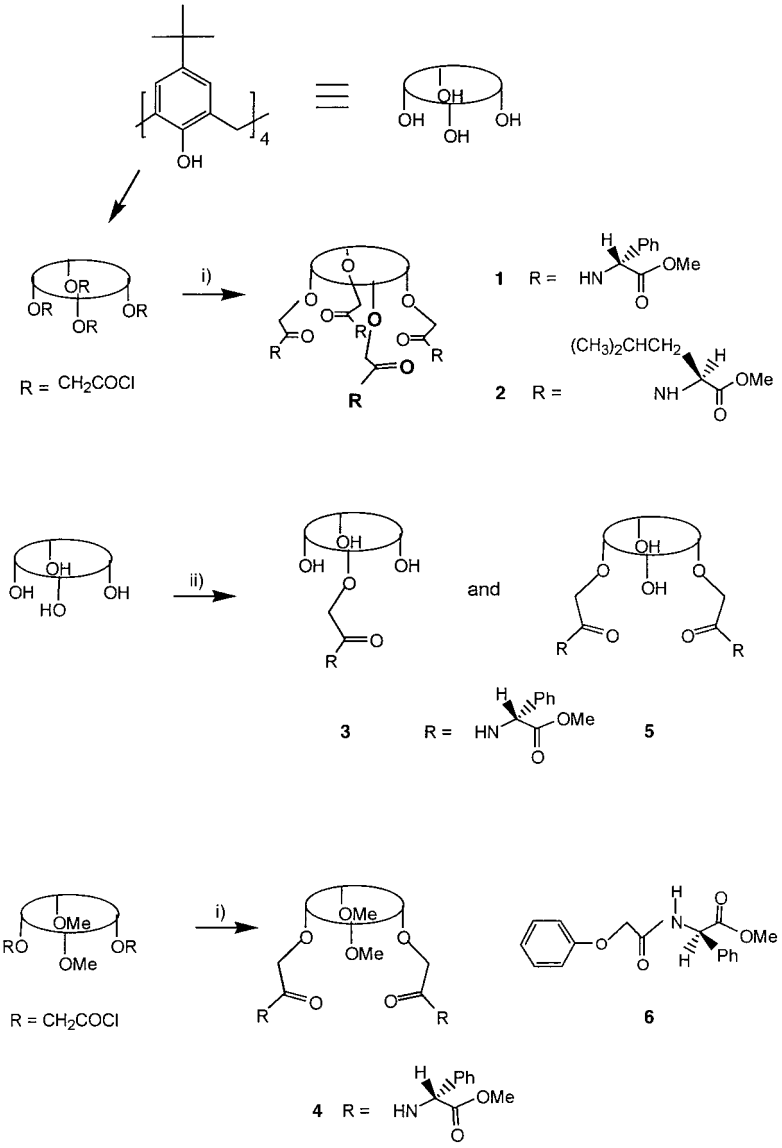

Scheme 1. Reagents and conditions: i) *R*-PhgOMe · HCl, or (*S*)-LeuOMe, Et_3N, CH_2Cl_2, RT; ii) *N*-(chloroacetyl)PhgOMe, K_2CO_3, KI, dry acetone, reflux.

Abstract in Croatian: *Sintetizirani su derivati Kaliks[4]arena s četiri O-(N-acetil-PhgOMe), (**1**), (Phg označava R-fenilglicin) ili O-(N-acetil-LeuOMe) (**2**) lanca na donjem rubu Kaliksarenske košarice. Ustanovljeno je da oba derivata tvore stabilne stožaste konformacije u kloroformu s ne-kovalentno organiziranim šuljinama na donjem rubu kaliksarenske košarice. Šupljine nastaju tvorbom cirkularnih međulančanih vodikovih veza između amidnih skupina. Ovakva organizacija kod **1** i **2** utječe na njihovu selektivnost u ekstrakcijama i eksperimentima prijenosa metalnih kationa. Sintetizirani su i derivati Kaliks[4]arena s jednim (**3**) i dva (**5**) $OCH_2COPhgOMe$ lanca te derivat **4** s 1,3-OMe-2,4-($OCH_2COPhgOMe$) supstituentima na donjem rubu. Spoj **3** tvori u kloroformu stožastu konformaciju stabiliziranu cirkularnim vodikovim vezama dok spoj **4** daje dvije C_2 simetrične konformacije u ravnoteži nastale tvorbom suprotno usmjerenih $NH\cdots OCH_3$ vodikovih veza. Spoj **5** tvori u otopini i krutom stanju konformaciju s jedinstvenim motivom vodikovih veza. Motiv se sastoji od dvije trocentrične $NH\cdots O$ i dvije $OH\cdots O$ vodikove veze na donjem rubu koje ukrućuju Kaliksarensku košaricu u spljoštenoj stožastoj konformaciji. Kristalografska strukturna analiza spoja **1** otkriva molekulsku strukturu s C_2 simetrijom organiziranu u beskonačne lance pomoću intra- i inter-molekulskih vodikovih veza. Molekulske strukture kompleksa [**1**, Na^+]ClO_4 u otopini i krutom stanju su identične i odgovaraju C_4 simetričnoj stožastoj konformaciji.*

Results and Discussion

Synthesis: The well-established method for the synthesis of tetra-(*O*-acetic ester) or -(*O*-acetamide) calix[4]arene derivatives in the *cone* conformation is based on the use of NaH as a strong base and also on the templating effect of sodium cations.[7c] However, for the synthesis of **1** and **2**, such a strong

  0947-6539/00/0603-0443 $ 17.50+.50/0

base has to be avoided owing to facile racemisation of *R*-phenylglycine and *S*-leucine in strongly basic conditions.[15] Alternatively, the synthesis was reported of calix[4]arene tetra(*O*-acetyl) ester in a *cone* conformation by using a weaker base, potassium carbonate, and a large excess of ethyl bromoacetate in acetone.[16a, b] The attempted one-step synthesis of **1** under the latter conditions that starts from *p-tert*-butyl-calix[4]arene and *N*-(chloroacetyl)-PhgOMe (K_2CO_3, KI, dry acetone, reflux under nitrogen) yielded, even after 7 days, only the mixture of the monosubstituted **3** (9% yield) and disubstituted **5** (40% yield), which are separable by column chromatography (silica gel, 0–2% MeOH in CH_2Cl_2). The stepwise route via the known calix[4]arene tetraacetic acid and its chloride[16] and PhgOMe or LeuOMe hydrochlorides (Et_3N, CH_2Cl_2) gave **1** (71% yield) or **2** (47% yield). Calix[4]arene 1,3-OMe derivative **4** with two 2,4-*O*-(CH_2COPhgCOOMe) strands was prepared from a known 1,3-dimethyl-2,4-(CH_2COOEt) derivative and its acid chloride[17] and coupled with PhgCOOMe. Compound **4** was produced in 78% yield. Compound **6** was prepared from phenol and (±)-*N*-(chloroacetyl)PhgOMe in 50% yield.

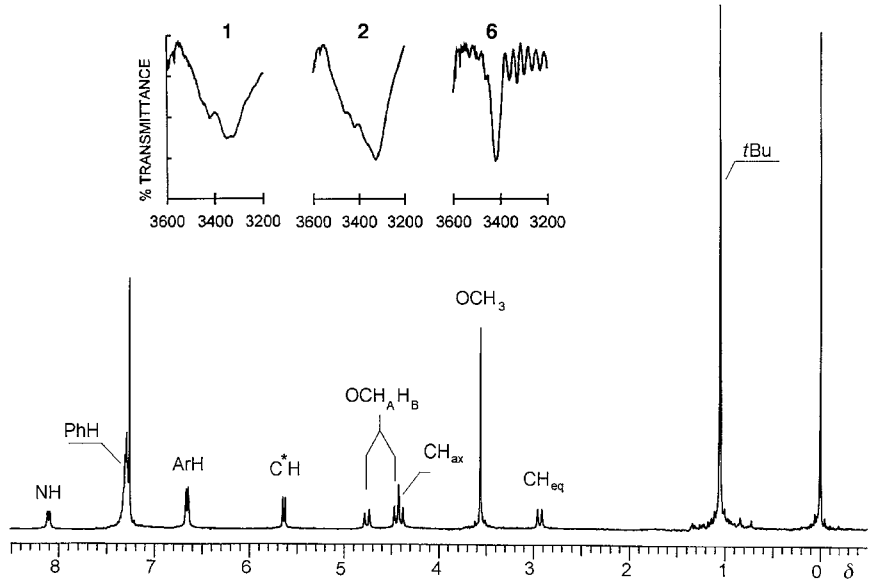

Figure 1. ^{1}H NMR ($CDCl_3$) of **1** and FTIR (inset, NH region; $CHCl_3$) spectra of **1**, **2** and **6**.

Solution conformations of calix[4]arene derivatives 1–5: intramolecular hydrogen bonding at the lower rim: ^{1}H NMR spectra of compounds **1** and **2** ($CDCl_3$) show the pattern characteristic of *p-tert*-butyl-calix[4]arene in a *cone* conformation,[7c] except for the appearance of two close singlets (δ = 6.66 and 6.68) of approximately equal intensity for the calix[4]arene aromatic protons (ArH) in the spectrum of **1** (Figure 1). Similar but more pronounced splitting of calixarene ArH protons was observed in amino acid derivatives with C_4 symmetry at the upper rim and was attributed to the presence of chiral amino acid units.[9] The NH protons of **1** ($\delta = 8.12$) and **2** ($\delta = 7.6$) are strongly shifted downfield relative to those of **6** ($\delta = 7.6$) and *N*-chloroacetyl-LeuOMe ($\delta = 6.94$); this indicates the involvement of the first two in hydrogen bonding (Table 1). In line with this observation, the high NH temperature coefficient[18] in $CDCl_3$ was determined for **1** ($\Delta\delta/\Delta T = 4.9 \times 10^{-3}$ K^{-1}; $c_1 = 8.1 \times 10^{-3}$ M), while for **6** at the same concentration the coefficient was only $\Delta\delta/\Delta T = 2.4 \times 10^{-3}$ K^{-1}, which is characteristic of non-hydrogen-bonded NHs exposed to chloroform. It was also observed that ^{1}H NMR spectra of **1** and **2** were concentration independent in the 10^{-4}–10^{-2} M range; this points to intramolecular hydrogen bonding in these compounds. Possible intrastrand hydrogen bonding to ether, amide or ester carbonyl oxygens as hydrogen-bond acceptors may be excluded as no such hydrogen bonding was observed for **6**. To identify the possible interstrand hydrogen-bond acceptors in **1** (ether, amide or ester carbonyl oxygens), the chemical shifts of carbonyl resonances in the ^{13}C NMR spectra of **1** ($\delta = 171.47$ and 169.65) and **6** ($\delta = 170.98$ and 167.75) were compared. The downfield shift ($\Delta\delta_{1,6} \approx 2$) of the higher field carbonyl resonance of **1** points to its involvement in hydrogen bonding. The assignment of carbonyl resonances in ^{13}C NMR spectra of **1** and **6** was achieved on the basis of deuterium isotope effects after partial NH–ND exchange. In accordance with literature data,[19] the larger two-bond isotope effects (75 ppb) and

Table 1. ^{1}H NMR NH and OH chemical shifts [ppm], temperature coefficients [$\Delta\delta/\Delta T \times 10^3$ K^{-1}], chemical shift difference of diastereotopic OCH_AH_B protons [$\Delta\delta_{OCHAHB}$, Hz], FTIR NH and amide I bands [ν, cm^{-1}], and corresponding H-bond types for calix[4]arene derivatives **1–5** and compound **6**.

Compound[a]	^{1}H NMR $CDCl_3$					FTIR		H Bond Type
	δ_{NH}	$\Delta\delta_{NH}/\Delta T$	$\Delta\delta_{OH}$	$\Delta\delta_{OH}/\Delta T$	$\Delta\delta_{OCHAHB}$	ν_{NH}	ν_{CONH}	
1	8.12	4.7	–	–	106	3351	1675	NH···O=CNH
2	7.60[b]	4.9	–	–	60	3326	1669	NH···O=CNH
3	9.70	3.5	9.80	4.7	14	3299[c]	1683	NH···OH, OH···OH; OH···OCH_2
			9.20	3.0				
			9.06	3.1				
4	8.20	3.8	–	–	32	3417	1683	NH···OCH_3
5	9.41	1.8	7.20	3.7	77	3316[c]	1676	NH···OCH_2, OH[d]; OH···OCH_2
6	7.60	2.4	–	–	14	3420	1686	–

[a] Concentration 8.1×10^{-3} M. [b] $\delta_{NH} = 6.94$ for *N*-chloroacetyl-LeuOMe in $CDCl_3$. [c] Combined OH and NH stretching bands. [d] NH in three-centred hydrogen bonding.

0947-6539/00/0603-0444 $ 17.50+.50/0 *Chem. Eur. J.* **2000**, *6*, No. 3

smaller three-bond effects (19.5 ppb) identified unequivocally the positions of amide (**1** $\delta = 169.65$; **6** $\delta = 167.75$) and ester (**1** $\delta = 171.47$; **6** $\delta = 170.98$) resonances. This identifies the amide carbonyls in **1** as hydrogen-bond acceptors. The FTIR data are fully in agreement with NMR results. In the spectra of **1** and **2** ($c = 3.5 \times 10^{-3}$ M, $CHCl_3$), the NH stretching bands at 3320–3350 cm^{-1} that correspond to hydrogen-bonded NHs are much stronger than those of free NH at 3420 cm^{-1}; the latter are, however, stronger in the spectrum of **6** (Figure 1, inset). Also, the amide I bands in the spectra of **1** and **2** appear at lower frequencies ($\nu = 1675$ and 1669 cm^{-1}, respectively) than that of **6** ($\nu = 1686$ cm^{-1}) in agreement with their participation in hydrogen bonding. The pronounced chemical shift difference ($\Delta\delta_{OCHAHB}$, Hz) of diastereotopic OCH_AH_B protons in the spectra of **1** and **2** (Table 1), which is absent in flexible derivative **6**, suggests the formation of rigid conformations of **1** and **2**. Thus, all the spectroscopic observations support the conclusion that in chloroform **1** and **2** exist in *cone* conformations with C_4 symmetry and are organised at the lower rim by interstrand hydrogen bonds (Figure 2). As expected for such a case, $\Delta\delta_{OCHA,HB}$ is strongly solvent dependent and diminishes with competitive hydrogen-bond-accepting power of solvent molecules ($\Delta\delta_{OCHA,HB}$ for **1** in $CDCl_3$, CD_3CN and [D_6]DMSO is 94, 25 and 0 Hz, respectively; for **6** in $CDCl_3$ 14 Hz; for **2** in $CDCl_3$ 60 Hz). Thus, in [D_6]DMSO the organisation at the lower rim completely disappears. Both ^{1}H and ^{13}C NMR spectra of **1** and **2** in $CDCl_3$ were found to be temperature independent in the 253–313 K range. The absence of any coalescence or even peak broadening features indicative of a time-averaged C_4 conformation suggests that **1** and **2** each exist as a stable conformation in $CDCl_3$. It should be noted that, depending on the left or right directionality of the NH···O=C bonding, two cyclodiastereoisomeric[20] conformations of **1** and **2** could be formed. However, only one species could be observed by NMR spectroscopy during the temperature variation, this implies the presence of only one cyclodiastereoisomer in solution.

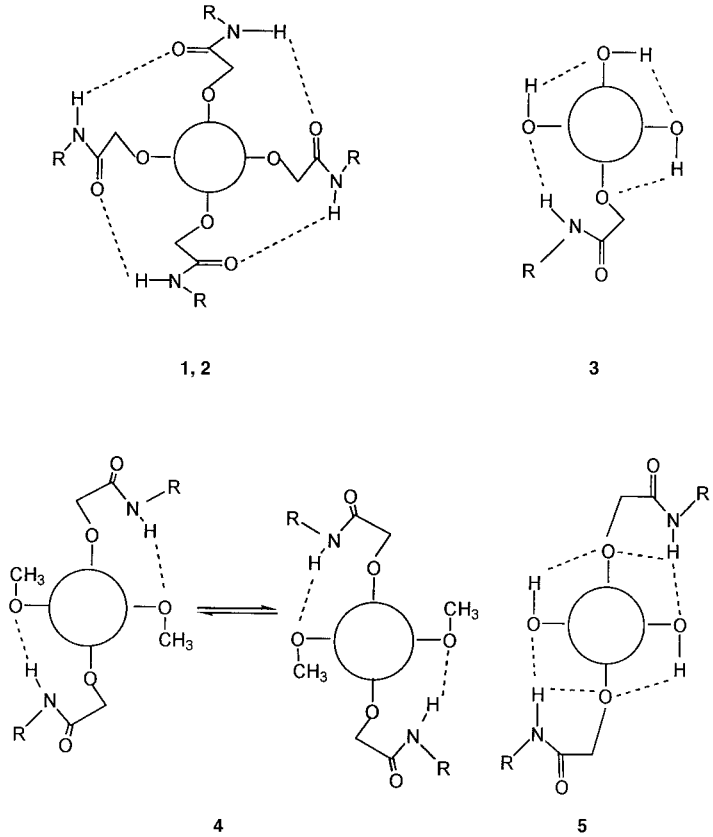

Figure 2. Lower rim hydrogen-bonding motifs for calix[4]arene derivatives **1**, **3**–**5** (R = PhgOMe) and **2** (R = LeuOMe) in solution.

The ^{1}H NMR spectrum of **3** ($CDCl_3$, RT; Table 1) with a single $O(CH_2COPhgOMe)$ strand shows sharp resonances for all protons. Diastereotopic equatorial and axial calixarene CH_2 protons give altogether five doublets due to the inherent asymmetry of **3**. The analysis of COSY maps shows that two axial protons of methylene groups attached to a strand with a phenolic unit appear at $\delta = 4.30$ and 4.07. These protons are coupled with two equatorial protons at $\delta = 3.51$ and 3.41. The two axial and two equatorial protons of the remaining methylenes give two proton doublets at $\delta = 4.11$ and 3.41, respectively (the latter overlap with a 1H doublet). At low field ($\delta = 9-10$), three sharp resonances for OH protons ($\delta =$ 9.80, 9.20 and 9.06) and one doublet for NH could be observed (Table 1). In the NOESY spectrum of **3**, the NOE effects between OH at $\delta = 9.80$ and those at $\delta = 9.20$ and 9.06, together with weak NOE interaction between NH and OH at $\delta = 9.02$, suggest their vicinal position at the lower rim of the calix[4]arene *cone*. Strong downfield shift of **3**-NH ($\delta = 9.70$ in $CDCl_3$) along with the high NH temperature coefficient (Table 1) suggest its participation in hydrogen bonding. In the FTIR spectrum, no free NH stretching band above 3400 cm^{-1} could be observed and the position of the amide I band at 1683 cm^{-1} suggests that the amide oxygen is not a hydrogen-bond acceptor. The analysis of OH proton chemical shifts and their temperature coefficients suggests that all three are involved in intramolecular hydrogen bonding and that the OH proton with the highest chemical shift ($\delta = 9.80$) also exhibits the highest value for the OH temperature coefficient ($\Delta\delta_{OH}/\Delta T = 4.7 \times 10^{-3}$ K^{-1}). This can be explained by its participation in hydrogen bonding with neighbouring OH and NH. The lower rim circular hydrogen-bonding motif shown in Figure 2 can explain the summarised spectroscopic data for **3**.

In the ^{1}H NMR spectrum of **4** at room temperature, the resonances are considerably broadened, which indicates conformational interconversion. The chemical shift of NH protons ($\delta = 8.20$), their temperature coefficient (3.8×10^{-3} K^{-1}) and the fact that the chemical shifts are not dependent on concentration suggest their involvement in intramolecular hydrogen bonding. Comparison of FTIR ν_{NH} data for **4** and model compound **6** also points to participation of **4**-NHs in weak hydrogen bonding. However, the ν_{CONH} (1683 cm^{-1}) of **4** is close to that of **6** (1686 cm^{-1}); this indicates that the amide carbonyl oxygens of **4** are not hydrogen-bond acceptors. Consequently, the existence of two NH···OCH_3 intramolecular hydrogen bonds in **4** seems to be the most likely explanation. For the calix[4]arene moiety of **4**, the pattern of ^{1}H NMR resonances observed suggests the formation of a C_2 flattened *cone* conformation. This is supported by considerable upfield shifts of one *tert*-butyl singlet ($\delta = 0.82$) and one ArH singlet ($\delta = 6.42$) because of the more proximate position of two aromatic rings in such a

flattened *cone* conformation. In the NOESY map, the NOE interactions between ArH signals at $\delta = 7.14$ and 7.16 with that at $\delta = 6.42$ indicate their close proximity in the *cone* conformation. These findings and the observed $NH \cdots OCH_3$ hydrogen bonds exclude the possible 1,3-alternate *cone* of **4** as one of the interconverting conformations in equilibrium. The relatively small OCH_AH_B chemical shift difference (Table 1) of **4** relative to **1** and **2** suggests their similar chemical environment. In conclusion, the NMR and FTIR data may be best explained by interconversion between two C_2 symmetric conformations of **4** with the $NH \cdots OCH_3$ hydrogen bonds in opposite directions (Figure 2).

All resonances in the ^{1}H NMR spectrum of **5** are sharp and this indicates the presence of one stable conformation. In a similar way to **4**, the observed resonances of the calix[4]arene moiety in the spectrum of **5** are in agreement with the flattened *cone* conformation. In the NOESY spectrum, the cross peaks for NH/OH, OH/*axial* methylene and more deshielded ArH singlets/*equatorial* methylene protons are observed, which shows their proximity in the flattened *cone* of **5**. The NH resonance is strongly shifted downfield ($\delta = 9.41$); however, its temperature coefficient is unexpectedly small ($\Delta\delta/\Delta T = 1.8 \times 10^{-3}$ K^{-1}; Table 1) relative to that of **4** and all other studied calixarenes. The molecular structure of **5** (Figure 4), obtained by X-ray structural analysis (see the section on crystal structures), presents a hydrogen-bonding motif (Figure 2) that could explain most of the spectroscopic observations. It consists of two three-centred $NH \cdots O$ and two $OH \cdots O$ hydrogen bonds. Such a hydrogen-bonding scheme with each NH involved in three-centred bonding might explain their high downfield shift and, at the same time, the unexpectedly low temperature coefficient. Apparently, the latter could be a consequence of strong three-centred hydrogen bonding, which remains stable during the temperature variation (20–50 °C, $CDCl_3$) used for determination of the temperature coefficients. The presence of six hydrogen bonds at the lower rim of **5** would explain the formation of a very stable conformation in solution. Remarkably, the temperature variation from 40–120 °C produced only slight changes in the ^{1}H NMR spectra of **5** dissolved in $CDCl_2CDCl_2$, as well as some line broadening. Support for the same hydrogen-bonding motif in solution as the one found in the crystals comes also from the comparison of the OCH_AH_B chemical shift difference for similarly substituted **5** and **4**. The OCH_AH_B chemical shift difference for **5** (77 Hz) is more than two times larger than that for **4** (32 Hz) and this strongly suggests a much more fixed position of OCH_AH_B in **5** than in **4**. The fixed position in the former is made possible by simultaneous hydrogen bonding of OH ($\Delta\delta/\Delta T$ for OH is 3.7×10^{-3} K^{-1}, Table 1) and NH protons to the oxygen acceptor of the OCH_AH_B group. It is worthwhile comparing the calixarene ArH resonances in the spectra of **4** and **5**, which have a similar type of substitution but differ in conformational stability. In the spectrum of **4**, one broad ($\delta = 6.42$) and two poorly resolved singlets ($\delta = 7.14$ and 7.16) can be observed for the calixarene ArH protons as a consequence of time-averaged conformational exchange. Such a process is expected to diminish the nonequivalence between the diastereotopic ArH protons. However, in the spectrum of **5**, four singlets can be observed ($\delta = 6.79$, 6.84, 7.01 and 7.07) due to conformational rigidity, which enhances the nonequivalence between the diastereotopic pairs of calixarene ArH protons. In conclusion, the spectroscopic data are in accord with the hydrogen-bonding motif found in the crystal structure of **5**. This unique motif with two three-centred $NH \cdots O$ and two $OH \cdots O$ hydrogen bonds strongly stabilises the C_2-symmetric flattened *cone* conformation of **5** in solution. This also explains the formation of only monosubstituted **3** (9%) and disubstituted **5** (40%) but not the tetrasubstituted **1** in the described synthetic procedure, that starts from *p-tert*-butylcalix[4]arene and *N*-(chloroacetyl)PhgOMe.

Structures and stability constants for [1-Na]SCN and [1-K]SCN complexes in solution: ^{1}H NMR spectra of [**1**-Na]SCN in both $CDCl_3$ and CD_3CN differ considerably from those of free **1** in the same solvents. The complexation-induced shifts, defined as $\Delta\delta = \delta_{[\mathbf{1}\text{-}M^+]} - \delta_{\mathbf{1}}$ [ppm], were determined for both solvents and Na- and KSCN and are presented in Table 2. The strongest upfield shifts were observed for NH protons; this is apparently due to disappearance of the circular $NH \cdots O{=}C$ hydrogen-bond arrangement upon complexation. Formation of [**1**-Na]SCN and [**1**-K]SCN complexes was also studied by means of ^{1}H NMR titrations in CD_3CN, as both inorganic salts were sufficiently soluble in this solvent. While at a **1**/NaSCN molar ratio of 0.5 the separate resonances for the complex and free **1** are simultaneously present, only shifts and broadening of resonances are observed in the **1**-KSCN spectrum (see Supporting Information). This shows that **1** forms a strong kinetically stable complex with Na^+ with slow exchange kinetics on an NMR timescale. On the other hand, the complex with K^+ exhibits much faster equilibrium kinetics. The stability constants for [**1**-K]SCN and [**1**-Na]SCN complexes in the same solvent were determined spectrophotometrically from the MSCN induced changes in electronic absorption of calix[4]arene.[14b] The constants of 2.6×10^6 M^{-1} and 8.2×10^4 M^{-1} have been obtained in this way for **1**-NaSCN and **1**-KSCN complexes, respectively. Their ratio gives a Na^+/K^+ selectivity of 30. It is interesting to compare the complexation behaviour of **1** and calix[4]arene tetra-[*O*-(*N*,*N*-diethylacetamide] derivatives[14c] with a similar type of binding site for metal cations, towards Na^+ and K^+ in acetonitrile; however, the latter lacks NH so that hydrogen-bonded organisation at the lower rim is not possible. For the diethylacetamide derivatives, the log K_s values exceed 8.5 for both Na^+ and K^+. Apparently, the presence of organisation in **1** lowers the stability constants for the same cations by at least 2–4 orders of magnitude. This effect may be explained by the competition of the metal

Table 2. ^{1}H NMR complexation-induced shifts [$\Delta\delta = \delta_{[\mathbf{1}\text{-}M^+]} - \delta_{\mathbf{1}}$ in ppm] of selected protons for complexes [**1**-Na]SCN and [**1**-K]SCN in $CDCl_3$ and CD_3CN.

	NH	Calix–ArH	OCH_AH_B	Calix–CH_{ax}	Calix–CH_{eq}	OCH_3
1-Na^+/$CDCl_3$	–0.45	0.31	–0.24	–0.24	0.30	0.12
1-Na^+/CD_3CN	–0.52	0.28	–0.39	–0.50	0.14	0.13
1-K^+/CD_3CN	–0.68	0.26	–0.36	–0.34	0.11	0.08

0947-6539/00/0603-0446 $ 17.50+.50/0 *Chem. Eur. J.* **2000**, *6*, No. 3

cations with NHs for amide carbonyl oxygen sites in the complexation with **1**. The Na^+, which is known to fit better in such a cavity at the lower rim, is a better competitor than K^+. This is caused by considerably weaker binding of K^+ and hence the Na^+/K^+ selectivity is equal to 30. Competition between metal cations and hydrogen bonding may be a useful principle for the construction of selective cation receptors or carriers.

Crystal structures and stereochemistry of 1, 5 and the [1-Na]ClO_4 complex: The molecular structures of **1** (Figure 3) and **5** (Figure 4) revealed the distorted *cone* of an approximate C_2 symmetry (Table 3). It is characterised by a sequence

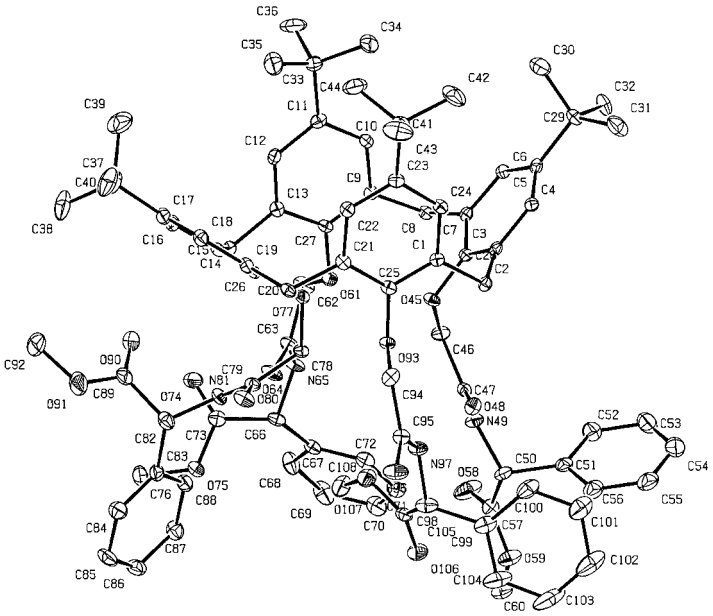

Figure 3. ORTEP drawing of **1** with thermal ellipsoids scaled at 30% probability. Only hydrogen atoms involved in hydrogen bonds are shown.

of the torsion angle signs $(+,-,+,-,+,-,+,-)$. To define the regularity of the cone, Ugozzoli and Andreetti[21] introduced a pair of torsional angles, ϕ and χ, about the methylene bonds of the macrocyclic ring. These are listed in Table 3. In the [**1**-Na]ClO_4 complex (Figure 5), the regular *cone* conformation of C_4 symmetry (with the crystallographic fourfold axis) was detected. Due to the high symmetry, the *cone* conformation is defined by a single pair of ϕ and χ values (Table 3). However, the terminal parts of the amino acid subunits disobeyed the C_4 crystallographic symmetry and disorder was encountered. Deformations of the *cone* are connected with the tilting of the phenyl rings towards the

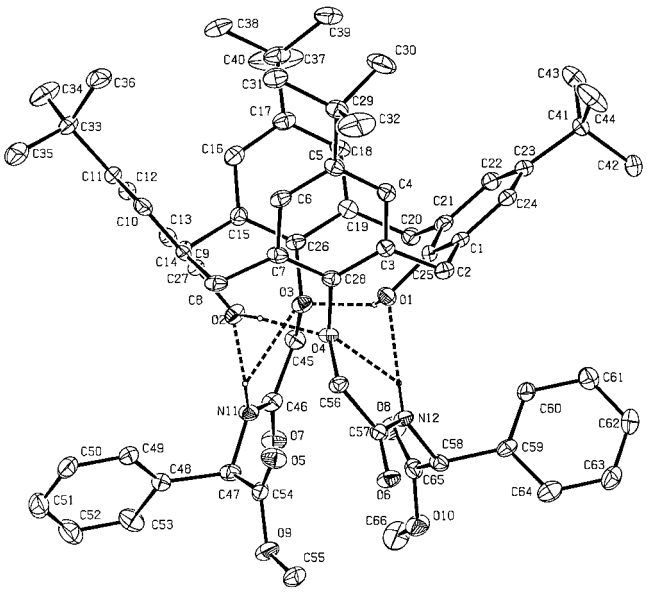

Figure 4. ORTEP drawing of **5** (thermal ellipsoids scaled at 30% probability) with intramolecular hydrogen bonds; only hydrogen atoms involved in hydrogen bonds are shown.

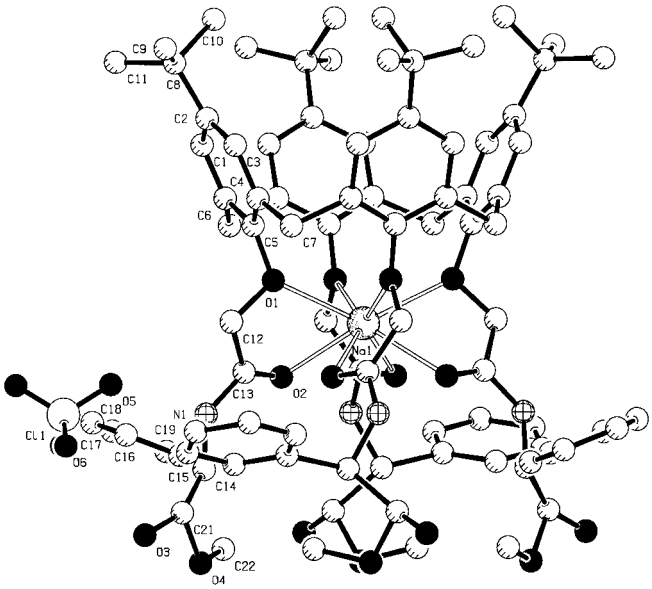

Figure 5. The [**1**-Na]ClO_4 complex with crystallographic fourfold symmetry. The coordination around Na^+ is regular square antiprism.

main molecular plane (defined with four methylene carbon atoms). In **1**, the two almost parallel phenyl rings, (C25-C1-C24-C23-C22-C21 and C27-C13-C12-C11-C10-C9), are almost perpendicular to the molecular plane [85.6(5)° and 85.7(3)°, respectively], whereas the other two (C28-C7-C6-C5-C4-C3 and C26-C19-C18-C17-C16-C15) are tilted away from the cavity; the angles between the main molecular plane

Table 3. Molecular conformations of **1**, **5** and [**1**-Na]ClO_4 defined by ϕ and χ parameters.[21] Esds are given in parentheses.

	ϕ_1 [°]	χ_1 [°]	ϕ_2 [°]	χ_2 [°]	ϕ_3 [°]	χ_3 [°]	ϕ_4 [°]	χ_4 [°]
1	89.5(5)	−60.0(6)	68.9(5)	113.1(5)	105.7(5)	−52.8(6)	62.2(5)	−98.4(4)
5	−76.6(6)	105.9(6)	−106.0(7)	80.5(7)	−78.6(7)	91.7(7)	−94.7(6)	75.9(7)
[1-Na]ClO_4	−76.1(8)	75.6(9)						

and these phenyl rings are 49.5(2)° and 36.9(2)°, respectively. These two phenyl rings are almost perpendicular to each other [85.4(2)°]. In **5**, two of the four hydroxy groups are substituted with amino acid chains and the orientation of the phenyl rings towards the main plane does not show such differences as in **1**; the angles between the phenyl rings (the sequence of atoms is the same as for **1**) and the main molecular plane are 39.8(2)°, 71.3(2)°, 51.2(2)° and 67.6(2)°, respectively. In [**1**-Na]ClO_4, the sodium ion is located on the crystallographic fourfold axis. The coordination polyhedron around Na^+ is a regular square antiprism, which is formed by four ether and four carbonyl oxygen atoms from four amino acid subunits with Na–O bond lengths of 2.465(9) and 2.471(5) Å. The dimensions of the calixarene baskets in **1**, [**1**-Na]ClO_4 and **5** do not leave sufficient room for a guest molecule. Around the fourfold axes, there is a disordered methanol molecule with a Na···O separation distance of 4.31 Å. However, the crystal lattice of **5** includes disordered solvent molecules.

The crystal packing of **1** is characterised by a two-dimensional hydrogen-bond network with infinite chains along *a* (Figures 3 and 6, Table 4); this is achieved through the intermolecular hydrogen bonds of N49-H···O96 and N65-H···O80. The remaining two donors, N81-H and N97-H, participate in intramolecular, interstrand hydrogen bonds. Two donors, N97-H and N49-H, are involved in three-centred hydrogen bonds with somewhat different functions in the crystal packing. N97-H forms an intrastrand hydrogen bond to O93 and an intramolecular, interstrand hydrogen bond to O48. The donor N49-H participates in an intrastrand interaction with O58 and an intermolecular one with O96. In the crystal lattice, the packing pattern reveals pronounced separation of the hydrophilic regions of amino acid subunits and hydrophobic ones with *tert*-butyl groups. The crystal structure of **5** reveals a circular intramolecular hydrogen-bond arrangement (Figure 4, Table 5) only. Two unsubstituted hydroxy groups are available, both as donors and acceptors. Both amide nitrogens, N11 and N12, are involved in the three-centred hydrogen bonds: N11-H to intrastrand ether oxygen O3 and to hydroxyl O2-H and N12-H repeats the same type of interaction to intrastrand ether oxygen O4 and to hydroxyl O1-H. The hydroxy groups act as donors to ether oxygen atoms (O1-H···O3 and O2-H···O4) to complete a circular hydrogen-bond arrangement, which is in the form of a twisted hexagonal ring (Figure 4). Due to the high disorder of solvent molecules in the crystal lattices of **5** and [**1**-Na]ClO_4, no firm conclusion about the details of their interaction can be given. In the crystal packing of [**1**-Na]ClO_4, the hydrogen bond N1-H···O5 (2.93(2) Å) connects a complex cation and a perchlorate anion.

Table 5. Hydrogen-bond geometry in **5**. (Esds are given in parentheses.)

	D–H···*A* [Å]	*D*–H [Å]	H···*A* [Å]	*D*–H···*A* [°]
N12-H···O1[a]	3.085(6)	0.86	2.23	174
N12-H···O4[a]	2.653(6)	0.86	2.26	108
N11-H···O2[a]	3.062(6)	0.86	2.20	176
N11-H···O3[a]	2.707(6)	0.86	2.36	105
O2-H···O4	2.850(5)	0.82	2.04	173
O1-H···O3	2.769(5)	0.82	2.05	147

[a] Three-centred H bonds.

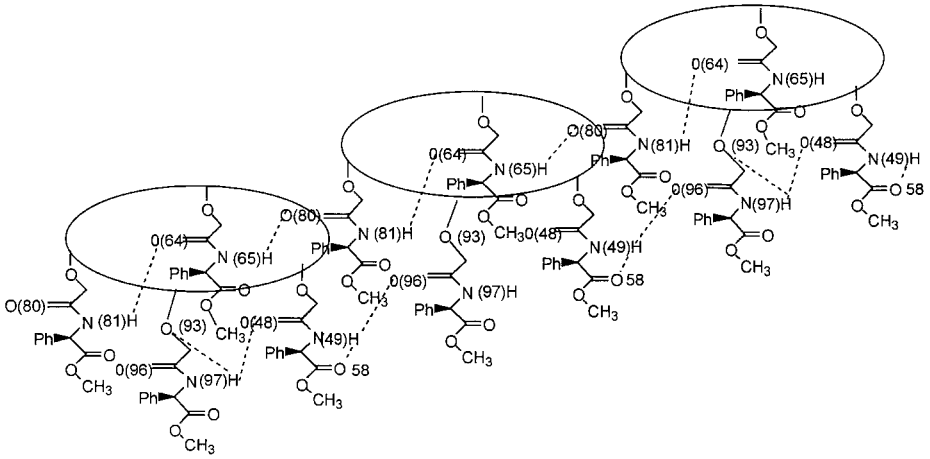

Figure 6. Scheme of intramolecular and intermolecular hydrogen bonds in **1**. Crystal packing of **1** with a two-dimensional hydrogen-bond network. Intramolecular hydrogen bonds are between two amino acid subunits. Intermolecular hydrogen bonds connect molecules along *a* into infinite chains, which are separated by the hydrophobic regions of Ph and *t*Bu groups.

Table 4. Hydrogen-bond geometry in **1**. (Esds are given in parentheses.)

	D – H···*A* [Å]	*D* – H [Å]	H···*A* [Å]	*D*–H···*A* [°]	Symmetry operations on *A*
N49-H···O58[a]	2.709(6)	0.86	2.38	103	*x*, *y*, *z*
N49-H···O96[a]	2.975(5)	0.86	2.20	149	$-1+x$, *y*, *z*
N65-H···O80	3.003(4)	0.86	2.17	164	$-1+x$, *y*, *z*
N81-H···O64	3.023(4)	0.86	2.17	170	*x*, *y*, *z*
N97-H···O48[a]	2.859(4)	0.86	2.17	137	*x*, *y*, *z*
N97-H···O93[a]	2.686(4)	0.86	2.31	107	*x*, *y*, *z*

[a] Three-centred H bonds.

Extraction and transport: The construction principle of **1** and **2** involves cation binding functionalities (four ether and four carbonyl oxygens), which are known to cooperatively bind metal cations in complexes of calix[4]arene tetra-(*O*-acetamide) derivatives.[14, 22] For **1** and **2**, however, organisation at the lower rim by circular amidic hydrogen bonds was observed in lipophilic solvents, when the amide carbonyl oxygens act as hydrogen-bond acceptors. Therefore, extraction and transport of alkaline metal cations by **1** and **2** are expected to be affected by the observed organisation. The results of extraction and transport studies with

0947-6539/00/0603-0448 $ 17.50+.50/0 *Chem. Eur. J.* **2000**, *6*, No. 3

1 and **2** are compared with those of previously studied calix[4]arene primary-[14a] and tertiary-acetamide[14c] derivatives that possess closely related binding sites. The experiments were performed under the same conditions as used with tetra-(*O*-acetamide) derivatives[22] so that comparison of the results was possible. The same experiments were performed with compound **4** with two $CH_2COPhgOMe$ strands; this produced a different organisation at the lower rim compared with **1** and **2**.

The results of extraction experiments (Table 6) show that **1** and **2** moderately extract Na-picrate and only weakly extract other alkaline picrates from water to the dichloromethane phase. The results were compared with those for calix[4]arene tetra-(*O*-acetamide) derivatives (% extraction: $Li^+ < 1$, Na^+ 2.7, $K^+ < 1$, Rb^+ 5.2 and Cs^+ 3.1)[14a] and calix[4]arene tetra-[*O*-(*N*,*N*-diethylacetamide)] derivatives (% extraction: Li^+ 62.5, Na^+ 95.5, K^+ 73.7, Rb^+ 24.0 and Cs^+ 11.8).[14c] This shows that **1** and **2** are better extractants than the former and much weaker than the latter. However, **1** and **2** exhibited higher Na^+/K^+ extraction selectivities (**1**, 8.9 and **2**, 6.7) than both the calix[4]arene primary ($Na^+/K^+ \geq 2.7$) and tertiary acetamide derivatives ($Na^+/K^+ = 1.3$). The phenylglycine derivative **1** showed better extraction and higher Na^+/K^+ selectivity than leucine derivative **2**. However, both ligands exhibited clear Na^+ selectivity among the tested alkaline picrates.

Table 6. The percentages of M-picrate extraction [$\log K_{ex}$] and transport rates of Na- and K-thiocyanates [$\mu mol\,h^{-1}\,cm^{-2}$[a]] for **1**, **2**, and **4**.

	% extraction [$\log K_{ex}$]					transport	
	Li^+	Na^+	K^+	Rb^+	Cs^+	Na^+	K^+
1	0.95	16.1; (6.6)	1.8; (5.6)	1.3	0.9	2.9	0.3
2	0.66	8.1; (6.2)	1.2; (5.3)	1.3	0.7	2.1	0.2
4	1.2	5.4; (6.0)	6.3; (6.1)	2.7	1.5	1.1	1.3

[a] Obtained by dividing the transport rates [$\mu mol\,h^{-1}$] by the surface area (4.23 cm^2) of the organic phase.

Derivative **4** with two $CH_2COPhgOMe$ strands and two OMe groups at the lower rim is a weaker and less selective extractant than **1** and **2**. In fact, **4** showed a slight preference for K^+ over Na^+ and slightly enhanced extraction of Li^+, Rb^+ and Cs^+ relative to **1** and **2**. Apparently, **4** with two $OCH_2COPhgOMe$ strands possesses a more flexible binding cavity than **1** and **2**, which both have four identical strands at the lower rim. Therefore, diminished Na^+/K^+ selectivity and somewhat better extraction of smaller Li^+ and larger Rb^+ and Cs^+ cations were observed for **4**.

In transport experiments (Table 6), dramatic differences between **1** and **2** and calix[4]arene tetra-[*O*-(*N*,*N*-diethylacetamide)] derivatives were observed. For example, **1** has a transport rate for Na^+ and reversed Na^+/K^+ selectivity (Na^+/K^+ selectivity: **1**, 9.6 and **2**, 10.5) that is more than 150 times higher than that for *N*,*N*-diethylacetamide derivatives (transport rate: Na^+ 0.04, K^+ 0.56 $\mu mol\,h^{-1}\,cm^{-2}$; K^+/Na^+ selectivity 14).[14c] It is well known that there is a bell-shaped dependence of cation transport rates on K_{ex} values of calix[4]arene ester and amide derivatives.[21] Comparison of the extraction equilibrium constants for **1** and **2** (Table 6) with those for *N*,*N*-diethylacetamide derivatives ($\log K_{ex}$: Na^+ 11.2, K^+ 8.8)[23] shows that the presence of the circular hydrogen-bond arrangement strongly reduces their extraction efficacy. This effect, as in the case of complexation in acetonitrile (preceding paragraph), should be the consequence of the competition between cation and amide NHs for amide carbonyl oxygen sites. Consequently, K_{ex} values for **1** and **2** are considerably lower than those for non-hydrogen-bonded diethylacetamide derivatives in which such competition is absent. However, the K_{ex} values determined for **1** and **2** seem to be more favourable for efficient transport to occur; this makes both **1** and **2** much better carriers than calixarene diethylacetamide derivatives. In conclusion, the presence of hydrogen-bonded organisation in **1** and **2** and the resulting competitive effects make their properties more like those of a carrier. In contrast, the *N*,*N*-diethylamide derivative, which is unable to form intramolecular hydrogen bonds at the lower rim, behaves as a typical receptor for the same cations.

Conclusion

Experimental evidence for molecular organisation in solution and in the crystal is available for **1**–**5** and the [**1**-Na]ClO_4 complex. According to the behaviour in solution, two groups were recognised: a) **1**, **2** and **3** and b) **4** and **5** (Figure 2). In apolar solvents ($CDCl_3$, CD_3CN), **1** and **2** with four strands of peptidic units and **3** with one such strand and three free OH groups formed a *cone* conformation with a circular hydrogen-bond arrangement at the lower rim. Spectroscopic data of **4** are in agreement with the time-averaged C_2 symmetric conformation formed by two intramolecular $NH\cdots OCH_3$ hydrogen bonds. In the crystal, four intramolecular hydrogen bonds (two are three-centred) were found for **5**. The spectroscopic data determined for **5** in $CDCl_3$ are in accord with the hydrogen-bonding motif found in the crystalline state. This motif keeps **5** in the flattened *cone* conformation in solution and in the solid state. The organisation is so stable that it overcomes concurrent intermolecular hydrogen-bonding motifs possible both in solution and in the solid state. In contrast, the high C_4 symmetric organisation of **1** in solution is reduced to C_2 in the crystal due to the occurrence of intermolecular hydrogen bonds. In the crystal that includes a polar environment, the hydrogen-bond donor/acceptor functionalities within one molecule compete with those of their neighbouring molecules. In addition to intramolecular hydrogen bonds, there are also intermolecular ones, which prevent the formation of the circular hydrogen-bond arrangement found in solution. Complexation of **1** with Na^+ makes the molecule more rigid and it keeps C_4 symmetry in the solid state and in solution. In the synthesis of **1**, the phenylglycine with the *R*-configuration was used. Thus, the chirality of the amino acid used dictates the orientation of the strands in the calixarene molecule; in the structure studied, it is in a clockwise direction. The presence of a circular hydrogen-bonding motif in **1** and **2** with the amide oxygen sites considerably influences their binding properties toward Na^+ and K^+. Compared with the calix[4]arene *N*,*N*-diethylacetamide derivatives with similar but non-hydrogen-bonding sites, the equilibrium extraction constants for **1** and **2** are three to five orders of magnitude

lower. This appeared to be a consequence of the competition between cations and amide NHs for amide carbonyl oxygen sites in **1** and **2**. However, the same competing process gives a lower but more favourable K_{ex} value for Na^+ transport. Consequently, the transport rate for **1**/Na^+ is more than 150 times higher than that found for the non-hydrogen-bonded *N*,*N*-diethylacetamide derivatives and the same cation.

In conclusion, we have presented evidence that the calix[4]arenes substituted at the lower rim with amino acids possess various types of intra- and intermolecular organisations in solution and in the solid state. The variety of the hydrogen-bonding motifs that occur in the studied calix[4]-arene derivatives may be of considerable importance for the future design of novel calix[4]arene-based receptors, carriers or supramolecular solid-state structures.

Experimental Section

General: Melting points were determined on the Kofler stage and were uncorrected. ^{1}H and ^{13}C NMR spectra were recorded with a Gemini 300 spectrometer (TMS was used as an internal standard) at 300 MHz and 75 MHz, respectively. In the description of ^{1}H and ^{13}C NMR spectra, the calixarene aromatic protons and carbon atoms were designated as ArH and ArC, respectively, and those of the phenylglycine phenyl group as PhH and PhC, respectively. IR and FTIR spectra were recorded on a Perkin Elmer P-E 2000 instrument. UV/Vis measurements were made with Cary 5 and PU 8730 UV/Vis spectrophotometers. Optical rotations were measured on an Optical Activity AA 10 automatic polarimeter at the wavelength of 589.3 nm. TLC was performed on silica gel Merck 60 F_{254} plates and column chromatography was carried out with 230–240 mesh Merck 60 silica gel. All chemicals were of the best grade commercially available and were used without purification. Solvents were purified according to standard procedures; dry solvents were obtained according to literature methods and stored over molecular sieves.

5,11,17,23-Tetra-*tert*-butyl-26,28,25,27-tetrakis-(*O*-methyl-*R*-α-phenylglycylcarbonylmethoxy)calix[4]arene (1): Triethylamine (0.36 mL, 2.61 mmol) was added to the cooled (−10 °C) solution of *R*-phenylglycine methyl ester hydrochloride (0.48 g, 2.24 mmol) in dry CH_2Cl_2 (30 mL) and stirred for 30 min. Then, the acid chloride of calix[4]arene tetracetic acid (the cone conformer)[22] (0.45 g, 0.47 mmol) in dry CH_2Cl_2 (30 mL) was added at once with a syringe. The reaction mixture was allowed to warm up to room temperature and was stirred for an additional 2 hours. After filtration, the filtrate was washed with NaOH (1.0 M), hydrochloric acid, brine and water. After drying and evaporation of the solvent, the product was crystallised from methanol, which gave **1** (0.49 g, 71 %). $R_f = 0.28$ (5 % MeOH/CH_2Cl_2); m.p. 255–256 °C; $[\alpha]_D^{20} = -62.0$ ($c = 1$ in CH_2Cl_2); ^{1}H NMR (300 MHz, $CDCl_3$, 20 °C, TMS): $\delta = 8.12$ (d, $^3J = 7.5$ Hz, 4H; NH), 7.30–7.27 (m, 20H; PhgH), 6.68 (s, 4H; ArH), 6.66 (s, 4H; ArH), 5.7 (d, $^3J = 7.5$ Hz, 4H; C*H), 4.75 (AB-d, $^2J = 13.5$ Hz, 4H; OCH_2CO), 4.41 (AB-d, $^2J = 13.5$ Hz, 4H; OCH_2CO), 4.46 (AB-d, $^2J = 13$ Hz, 4H; $ArCH_2Ar$), 3.58 (s, 12H; OMe), 2.95 (AB-d, $^2J = 13$ Hz, 4H; $ArCH_2ArH$), 1.07 (s, 36H; CMe_3); ^{13}C NMR (75 MHz, $CDCl_3$, 20 °C): $\delta = 171.47$ (*C*OOMe), 169.64 (*C*ONH), 153.16 (*para*-Ar−*C*), 145.155 (Ar−*C*), 136.35 (Ph−*C*), 132.56 and 133.11 (*meta*-Ar−*C*), 128.66 (*ortho*-Ph−*C*), 128.22 (*meta*-Ph−*C*), 127.87 (*para*-Ph−*C*), 125.26 and 125.63 (*ortho*-Ar−*C*), 74.0 (OCH_2CO), 55.9 (C*H), 52.4 (O*Me*), 33.58 (*C*-*tert*-butyl), 31.5 ($ArCH_2Ar$), 31.12 (CH_3-*tert*-butyl); FTIR ($c = 5 \times 10^{-3}$ M, CH_2Cl_2): $\tilde{\nu} = 3422$ (w) and 3351 (s) (NH), 1744 (COOMe), 1675 (CONH, amide I), 1521 cm^{-1} (CONH, amide II); $C_{88}H_{100}N_4O_{16}$ (1469.8): calcd C 71.91, H 6.86, N 3.81; found C 71.89, H 6.87, N 3.81.

5,11,17,23-Tetra-*tert*-butyl-26,28,25,27-(*O*-methyl-*S*-α-leucil-carbonylmethoxy)calix[4]arene (2): This compound was prepared as described for **1** from the methyl ester of *S*-leucine hydrochloride (0.95 g, 5.23 mmol) and acid chloride of calix[4]arene tetraacetic acid (the cone conformer)[23] (1.19 mmol). Recrystallisation from methanol gave **2** (0.93 g, 56 %). $R_f = 0.34$ (5 % MeOH/CH_2Cl_2); m.p. 322–323 °C, $[\alpha]_D^{20} = -32.0$ ($c = 1$ in CH_2Cl_2); ^{1}H NMR (300 MHz, $CDCl_3$, 20 °C, TMS): $\delta = 7.67$ (br d, 4H; NH), 6.76 (s, 8H; ArH), 4.70 (AB-d, $^2J = 12.8$ Hz, 4H; $ArCH_2Ar$), 4.65–4.72 (m and AB-d, 8H; OCH_2COO), 4.54 (AB-d, $^2J = 14.0$ Hz, 4H; OCH_2COO), 3.69 (s, 12H; OMe), 3.19 (AB-d, $^2J = 12.8$ Hz, 4H; $ArCH_2$-Ar), 1.59–1.61 (m, 12H; CH_2CH), 1.07 (s, 36H; *t*Bu), 0.88 (m, 24H; CH_3); ^{13}C NMR (75 MHz, $CDCl_3$, 20 °C): $\delta = 173.87$ (*C*OOMe), 170.12 (*C*ONH), 153.11 (*para*-Ar−*C*), 145.25 (Ar−*C*), 132.47 and 133.46 (*meta*-Ar−*C*), 125.25 and 125.64 (*ortho*-Ar−*C*), 74.07 (OCH_2CO), 51.97 (OCH_3), 50.30 (*C**), 40.39 (Leu−*C*), 33.60 (*C*-*tert*-butyl), 31.75 ($ArCH_2Ar$), 31.13 (*C*-*tert*-butyl), 24.47 (Leu−*C*H), 21.40 and 22.47 (Leu−CH_3); FTIR ($c = 5 \times 10^{-3}$ in CH_2Cl_2): $\tilde{\nu} = 3423$ (w) and 3326 (s) (NH), 1746 (COOMe), 1669 (CONH, amide I), 1541 cm^{-1} (CONH, amide II); $C_{80}H_{116}N_4O_{16}$ (1389.8): calcd C 69.14, H 8.41, N 4.03; found C 69.33, H 8.20, N 4.22.

5,11,17,23-Tetra-*tert*-butyl-25,27-dihydroxy-26,28-bis-(*O*-methyl-*R*-α-phenylglycylcarbonylmethoxy)calix[4]arene (5) and 5,11,17,23-tetra-*tert*-butyl-25,27,26-trihydroxy-28-(*O*-methyl-*R*-α-phenylglycylcarbonyl-methoxy)calix[4]arene (3): A mixture of *p*-*tert*-butyl-calix[4]arene (0.5 g, 0.77 mmol), potassium carbonate (212.5 mg, 1.54 mmol), potassium iodide (281.5 mg, 1.69 mmol) and *N*-chloroacetyl-PhgOMe (361.0 mg, 1.54 mmol) in dry acetone (25 mL) was stirred and heated under reflux for 15 h. The cooled solution was filtered through a bed of Celite and the filtrate was combined with dichloromethane washings and evaporated to dryness. The residue was purified by column chromatography (silica gel/5 % CH_3OH in CH_2Cl_2 as eluent). Fractions with $R_f = 0.2–0.3$ were collected to give **5** after evaporation of the solvents. Recrystallisation from methanol gave the diester **5** (325 mg, 39.9 %). $R_f = 0.26$ (2 % MeOH/CH_2Cl_2); m.p. 146–147 °C; $[\alpha]_D^{20} = -29$ ($c = 1$ in CH_2Cl_2); ^{1}H NMR (300 MHz, $CDCl_3$, 20 °C, TMS): $\delta = 9.40$ (d, $^3J = 6.2$ Hz, 2H; NH), 7.35–7.23 (m, 10H; PhH), 7.20 (s, 2H; OH), 7.07 (s, 2H; ArH), 7.01 (s, 2H; ArH), 6.84 (s, 2H; ArH), 6.79 (s, 2H; ArH), 5.62 (d, $^3J = 6.2$ Hz, 2H; C*H), 4.44 (AB-d, $^2J = 15.2$ Hz, 2H; $ArCH_2Ar$), 4.21 (AB-d, $^2J = 15.5$ Hz, 4H; OCH_2CO), 4.19 (AB-d, $^2J = 15.5$ Hz, 4H; OCH_2CO), 3.77 (AB-d, $^2J = 13.5$ Hz, 2H; $ArCH_2Ar$), 3.69 (s, 6H; OMe), 3.39 (AB-d, $^2J = 13.4$ Hz, 2H; $ArCH_2Ar$), 3.25 (AB-d, $^2J = 13.48$ Hz, 4H; $ArCH_2Ar$), 1.28 (s, 18H; CMe_3), 0.97 (s, 16H; CMe_3); ^{13}C NMR (75 MHz, $CDCl_3$, 20 °C): $\delta = 170.91$ (*C*OOMe), 168.63 (*C*ONH), 149.49 and 147.97 (*para*-Ar−*C*), 149.31 and 142.50 (Ar−*C*), 135.29 (Ph−*C*), 132.31 and 131.82 (*meta*-Ar−*C*), 128.79, 128.54, 128.20, 128.00, 126.98, 126.44, 126.20, 125.92, 125.72, 125.51, 125.39, 125.16, 74.38 (OCH_2CO), 57.15 (C*H), 52.42 (O*Me*), 33.76 and 33.64 (*C*-*tert*-butyl), 31.88 and 31.82 ($ArCH_2Ar$), 31.41, 31.05 and 30.66 (CH_3-*tert*-butyl); FTIR ($c = 5 \times 10^{-3}$ M in CH_2Cl_2): $\tilde{\nu} = 3316$ (w) (OH, NH), 1743 (COOMe), 1676 (CONH, amide I), 1523 cm^{-1} (CONH, amide II); $C_{66}H_{78}N_2O_{10}$ (1059.36): calcd C 74.83, H 7.42, N 2.64; found C 74.62, H 7.39, N 0.862.

Compound 3: Fractions with $R_f = 0.5–0.6$ were collected to give **3** (59 mg, 9 %). $R_f = 0.55$ (2 % MeOH/CH_2Cl_2); m.p. 223–224 °C; $[\alpha]_D^{20} = -10$ ($c = 1$ in CH_2Cl_2); ^{1}H NMR (300 MHz, $CDCl_3$): $\delta = 9.79$ (s, 1H; OH), 9.70 (d, $^3J = 7.5$ Hz, 1H; NH), 9.20 (s, 1H; OH), 9.06 (s, 1H; OH), 7.59–7.28 (m, 5H; PhH), 7.23–6.97 (m, 8H; ArH), 5.86 (d, $^3J = 7.58$ Hz, 1H; C*H), 4.62 (AB-d, $^2J = 15$ Hz, 2H; OCH_2CO), 4.3 (AB-d, $^2J = 13$ Hz, 1H; $ArCH_2Ar$), 4.12 (AB-d, $^2J = 13$ Hz, 2H; $ArCH_2Ar$), 4.08 (AB-d, $^2J = 13$ Hz, 1H; $ArCH_2Ar$), 3.81 (s, 3H; OMe), 3.51 (AB-d, $^2J = 13.6$ Hz, 1H; $ArCH_2Ar$), 3.42 (AB-d, $^2J = 13.9$ Hz, 2H; $ArCH_2Ar$), 3.41 (AB-d, $^2J = 13.2$ Hz, 1H; $ArCH_2Ar$), 1.21 (s, 18H; CMe_3), 1.20 (s, 9H; CMe_3), 1.16 (s, 9H; CMe_3); ^{13}C NMR (75 MHz, $CDCl_3$, 20 °C): $\delta = 170.94$ (*C*OOMe), 167.85 (*C*ONH), 149.14, 148.60, 148.21, 148.12, 147.07, 143.90, 143.45, 135.67, 132.72, 129.2, 128.61, 128.25, 128.16, 128.10, 127.12, 126.94, 126.80, 126.72, 125.99, 125.77, 125.70, 75.17 (OCH_2CO), 56.74 (C*H), 52.63 (O*Me*), 34.09, 33.87 and 33.72 (*C*-*tert*-butyl), 32.64, 31.92 and 31.79 ($ArCH_2Ar$), 31.67, 31.32, 31.23 and 30.90 (CH_3-*tert*-butyl); FTIR ($c = 5 \times 10^{-3}$ M in CH_2Cl_2): $\tilde{\nu} = 3299$ (w) (OH, NH), 1748 (COOMe), 1683 (CONH, amide I), 1487 cm^{-1} (CONH, amide II).

5,11,17,23-Tetra-*tert*-butyl-25,27-di(*O*-methyl)-26,28-bis-(*O*-methyl-*R*-α-phenylglycylcarbonylmethoxy)calix[4]arene (4): Triethylamine (0.178 mL, 1.27 mmol) was added to the cooled (−10 °C) solution of *R*-phenylglycine methyl ester hydrochloride (0.247 g, 1.15 mmol) in dry CH_2Cl_2 (20 mL) and stirred for 30 min. Then, the acid chloride of calix[4]arene diacetic acid[17] (0.435 g, 0.52 mmol) in dry CH_2Cl_2 (20 mL) was added at once and the reaction mixture was allowed to warm up to room temperature and was stirred for 2 hours. After filtration, the filtrate was washed with NaOH (1.0 M), hydrochloric acid, brine and water. After drying and evaporation of

0947-6539/00/0603-0450 $ 17.50+.50/0 *Chem. Eur. J.* **2000**, *6*, No. 3

the solvent, the crude product was crystallised from methanol and **4** was produced (0.423 g, 78%). $R_f = 0.4$ (5% MeOH/CH_2Cl_2); m.p. 240–241 °C; $[\alpha]_D^{20} = -62.0$ ($c = 1$ in $CHCl_3$); ^{1}H NMR (300 MHz, $CDCl_3$, 20 °C, TMS): $\delta = 8.15$ (br d, 2H; NH), 7.51–7.28 (m, 10H; PhH), 7.16 (s, 2H; ArH), 7.14 (s, 2H; ArH), 6.42 (s, 4H; ArH), 5.84 (d, $^3J = 5.8$ Hz, 2H; C*H), 4.24–4.15 (AB, 4H; $ArCH_2Ar$ and AB 4H; OCH_2CO), 4.07 (s, 6H; ArOMe), 3.26–3.14 (m-AB, 4H; $ArCH_2Ar$), 1.35 (s, 18H; CMe_3), 0.82 (s, 18H; CMe_3); ^{13}C NMR (75 MHz, $CDCl_3$, 20 °C): $\delta = 170.81$ (*C*OOMe), 168.62 (*C*ONH), 155.17 (*para*-Ar–*C*), 151.61, 145.85 and 145.27 (Ar–*C*), 136.66 (Ph–*C*), 135.50 and 135.37 (*meta*-Ar–*C*), 131.08, 130.95, 128.95 (*ortho*-Ph–*C*), 128.54 (*meta*-Ph–*C*), 127.53 (*para*-Ph–*C*), 125.85, 125.85 and 124.79 (*ortho*-Ar–*C*), 74.06 (O*C*H_2CO), 60.76 (ArO*Me*), 55.61 (C*H), 52.50 (O*Me*), 34.00 and 33.42 (*C*-*tert*-butyl), 31.49 and 30.82 (CH_3-*tert*-butyl), 31.19, 30.60 and 30.56 (Ar*C*H_2Ar); FTIR ($c = 5 \times 10^{-3}$ M in CH_2Cl_2): $\tilde{\nu} = 3690$ (w) and 3417 (s) (NH), 1746 (COOMe), 1683 (CONH, amide I), 1509 cm^{-1} (CONH, amide II); $C_{68}H_{82}N_2O_{10}$ (1087.42): calcd C 75.11, H 7.60, N 2.58; found C 75.11, H 7.86, N 2.69.

Methyl *N*-(phenoxyacetyl)-*R*-phenylglycine (6): This compound was prepared from *N*-chloroacetyl-PhgOMe and phenol in the presence of *t*BuOK in dry benzene. Yield 50%. $R_f = 0.79$ (2% MeOH/CH_2Cl_2); m.p. 95–96 °C; ^{1}H NMR (300 MHz, $CDCl_3$, 20 °C, TMS): $\delta = 7.58$ (d, $^3J = 7.6$ MHz, 1H; NH), 7.27–7.35 (m, 7H; ArH), 6.93–7.06 (m, 3H; ArH), 5.65 (d, $^3J = 7.5$ Hz, 1H; C*H), 4.53 (AB-d, $^2J = 4.4$ Hz, 2H; OCH_2CO), 3.74 (s, 3H; OMe); ^{13}C NMR (75 MHz, $CDCl_3$, 20 °C): $\delta = 170.90$ (s, *C*ONH), 167.73 (s, *C*OOMe), 157.14 (Ph–*C*), 136.05 (Ph–*C*), 129.72 (Ph–*C*), 128.97 (Ph–*C*), 128.62 (Ph–*C*), 127.19 (Ph–*C*), 122.14 (Ph–*C*), 114.76 (Ph–*C*), 57.12 (O*C*H_2CO), 55.75 (*C**), 52.70 (O*Me*); FTIR ($c = 5 \times 10^{-3}$ M in CH_2Cl_2): $\tilde{\nu} = 3420$ (NH), 1744 (COOMe), 1686 (CONH, amide I), 1517 cm^{-1} (CONH, amide II); $C_{17}H_{17}NO_4$ (299.33): calcd C 68.22, H 5.72, N 4.68; found C 68.15, H 5.75, N 4.67.

Picrate extractions: Metal picrates (2.5×10^{-4} M) were prepared in situ by dissolving the metal hydroxide (0.01 mol) in picric acid (2.5×10^{-4} M, 100 mL). Distilled water was used for all aqueous solutions. Solutions (2.5×10^{-4} M) of the calixarene derivatives were prepared in dichloromethane. Equal volumes (5 mL) of the two solutions were shaken vigorously for 30 min in a 50 mL extraction flask. The solutions were left to stand until phase separation was complete. The concentration of picrate ion in the organic phase was then determined spectrophotometrically as described by Pedersen.[24] Control experiments showed that no picrate extraction occurred in the absence of a calixarene derivative.

Transport measurements: Thoman's[25] modification of the procedure described by Lamb et al.[26] was used to measure the rates of ion transport through a dichloromethane membrane. The membrane (CH_2Cl_2, 10 mL, 7×10^{-4} M of the calixarene derivative) was placed in a 70 mL beaker, which contained a magnetic stirring bar. A 20 mm diameter glass cylinder was inserted 10 mm into the CH_2Cl_2 solution and clamped securely into position. The source phase (3 mL, 5×10^{-2} M metal thiocyanate) was very slowly run down the inside of the cylinder. Similarly, the receiving phase (7 mL, 0.2 M $Fe(NO_3)_3$ in 0.2 M nitric acid) was run down the outside. The system was stirred slowly at approximately 100 rpm. Samples were withdrawn from the receiving phase at 1 h intervals and the absorbance recorded at $\lambda_{max} = 480$ nm for $Fe(SCN)^{2+}$. The ε value of 4400 $L\,mol^{-1}\,cm^{-1}$ was used for calculations. The experiment, when performed in the absence of calixarene, showed no transport of metal thiocyanate.

Preparation of complexes: The calixarene derivative **1** (100 mg) was suspended in methanol (20–30 mL) and the mixture was heated until a homogeneous solution was obtained. The Na-thiocyanate (3 equiv) was added and the mixture was heated again until homogeneous and filtered. The solution was then allowed to cool slowly to room temperature. After several days, the crystals of the [**1**-Na]SCN complex were collected and recrystallised from the same solvent. The same procedure applied for **1** and KSCN failed to give the complex. However, the formation of the [**1**-K]SCN complex in CD_3CN was observed by NMR spectroscopy (see Supporting Information).

5,11,17,23-Tetra-*tert*-butyl-26,28,25,27-tetrakis-(*O*-methyl-*R*-α-phenylglycylcarbonylmethoxy)calix[4]arene-NaSCN complex [1-Na]SCN: ^{1}H NMR (300 MHz, $CDCl_3$, 20 °C, TMS): $\delta = 7.45$ (br s, 4H; NH), 7.44–7.28 (m, 20H; Ph and ArH), 6.99 (br s, 8H; ArH), 5.62 (d, $^3J = 6.7$ Hz, 4H; C*H), 4.49 (AB-br d, $^2J = 14.0$ Hz, 4H; OCH_2CO), 4.30 (AB-br d, $^2J = 14.0$ Hz, 4H; OCH_2CO), 4.22 (AB-d, $^2J = 10.5$ Hz, 4H; $ArCH_2Ar$), 3.70 (s, 12H; OMe), 2.95 (AB-d, $^2J = 10.5$ Hz, 4H; $ArCH_2Ar$), 1.09 (s, 36H; CMe_3); ^{13}C NMR (75 MHz, $CDCl_3$, 20 °C): $\delta = 171.29$ (*C*OOMe), 169.55 (*C*ONH), 150.04 (*para*-Ar–*C*), 147.80 (Ar–*C*), 136.15 (Ph–*C*), 134.24 and 134.10 (*meta*-Ar–*C*), 132.37 (S*C*N-), 128.87 (*ortho*-Ph–*C*), 128.66 (*meta*-Ph–*C*), 127.61 (*para*-Ph–*C*), 125.72 and 125.61 (*ortho*-Ar–*C*), 74.33 (O*C*H_2CO), 56.60 (C*H), 52.89 (O*Me*), 33.82 (*C*-*tert*-butyl), 29.99 (Ar*C*H_2Ar), 30.99 (CH_3-*tert*-butyl); FTIR ($c = 5 \times 10^{-3}$ M in CH_2Cl_2): $\tilde{\nu} = 3413$ (w) and 3330 (s), 2050 (SCN^-) (NH), 1742 (COOMe), 1697 and 1684 (CONH, amide I), 1522 cm^{-1} (CONH, amide II).

Crystal structure determination of 1, 5 and [1-Na]ClO_4: The crystallisation of samples required great attention. Crystallisation from a hot solution of **1** in methanol resulted in well-formed but unstable crystals. It was discovered that a few drops of THF could stabilise the crystals. Therefore, vapour diffusion of methanol into a solution of **1** in THF at room temperature was used and good crystals for X-ray measurements were obtained. Crystals of **5** were obtained by slow evaporation from a mixture of dichloromethane and ethanol (1:1 vol) at 277 K. Good quality crystals of [**1**-Na]ClO_4 grew by using slow evaporation of a solution in ethanol. Crystals of **1**, **5** and [**1**-Na]ClO_4 were covered with protective grease and immediately inserted into the cold N_2 stream of the low-temperature device on the diffractometer. The crystallographic data and details of data collection and refinement have been listed in Table 7.[27–32] D-amino acids were used in synthesis and during structure determination chirality was assigned accordingly. Scattering factors used in calculations were from SHELXL97.[29] Hydrogen atoms were calculated on stereochemical grounds and refined using the SHELX97 riding model. The crystal structure of **5** revealed disordered solvent molecules (two water molecules with positional parameter = 0.5 (pp); two methanol molecules with pp = 0.5 and furfuraldehyde with pp = 0.25). Furfuraldehyde can be detected at a low concentration in ethanol; in the crystallisation procedure, the less volatile furfuraldehyde increased in concentration in the mother liquor. During purification of **5**, recrystallisations in methanol were used and the procedure applied can explain the small amount of disordered methanol in the crystal lattice. In the crystal structure of [**1**-Na]ClO_4, the terminal part of the amino acid subunits as well as *tert*-butyl groups revealed disorder and therefore these fragments were refined isotropically. Two crystalline water molecules, each with pp = 0.5, were found. In the space between chains, there was a disordered methanol molecule (pp = 0.25); oxygen and carbon atoms were located on a fourfold axis that was in disagreement with the entire molecular symmetry (CH_3OH). Structure determination in orthorhombic symmetry failed.

Crystallographic data (excluding structure factors) for the structures reported in this paper have been deposited with the Cambridge Crystallographic Data Centre as supplementary publication nos. CCDC-113248 (**1**), CCDC-113249 (**5**) and CCDC-113250 ([**1**-Na]ClO_4). Copies of the data can be obtained free of charge on application to CCDC, 12 Union Road, Cambridge CB2 1EZ, UK (fax: (+44) 1223-336-033; e-mail: deposit@ccdc.cam.ac.uk).

Acknowledgements

The financial support from the Croatian Ministry of Science and Technology (Programmes 009807 and 009806) is gratefully acknowledged.

[1] A. R. Fersht, *Trends Biochem. Sci.* **1987**, *28*, 3111.
[2] C. B. Gibb, A. R. Mezo, A. S. Canston, J. R. Fraser, F. C. S. Tsai, J. C. Sherman, *Tetrahedron* **1995**, *32*, 8719.
[3] R. Hirschmann, P. A. Sprengler, T. Kawasaki, J. W. Leahy, W. C. Shakespeare, A. B. Smith III, *Tetrahedron* **1993**, *49*, 3665.
[4] K. S. Akerfeldt, R. M. Kim, D. Camac, J. T. Groves, J. D. Lear, J. W. F. DeGrado, *J. Am. Chem. Soc.* **1992**, *114*, 9656.
[5] P. Dumy, I. M. Eggleston, S. Cervigni, U. Sila, X. Sun, M. Mutter, *Tetrahedron Lett.* **1995**, *36*, 1255.
[6] R. Hirshmann, K. C. Nicolau, S. Pietranico, E. M. Leahy, J. Salvino, B. Arison, M. Cichy, P. G. Spoors, W. C. Shakespeare, P. A. Sprengler, P.

Table 7. Crystallographic data, structure solution and refinement of **1**, **5** and [**1**-Na]ClO_4.

	1	**5**	[**1**-Na]ClO_4
formula	$C_{88}H_{100}N_4O_{16}$	$C_{66}H_{78}N_2O_{10}$	$[C_{88}H_{100}N_4O_{16}Na]ClO_4$
solvent	–	CH_3OH, 0.25; $C_4H_7O_2N$, H_2O	0.125 CH_3OH, H_2O
M_r	1469.78	1059.36	1592.24
crystal system	monoclinic	orthorhombic	tetragonal
space group	$P2_1$	$P2_12_12_1$	$P42_12$
a [Å]	9.8257(7)	15.5354(7)	15.005(1)
b [Å]	25.5700(8)	20.2015(8)	15.005(1)
c [Å]	16.6058(7)	22.340(1)	20.156(2)
β [°]	93.969(6)		
V [Å^3]	4162.1(4)	7011.0(5)	4538.2(1)
Z	2	4	1
ρ [mg m^{-3}]	1.176	1.0614	1.158
radiation	$Cu_{K\alpha}$	$Cu_{K\alpha}$	$Cu_{K\alpha}$
λ [Å]	1.54184	1.54184	1.54184
θ range [°] for cell determination	40.09 – 45.35	40.02 – 46.82	8.35 – 46.60
μ [mm^{-1}]	0.65	0.58	0.98
T [K]	105	107	107
crystal form	plate	prismatic	prismatic
crystal size [mm]	$0.07 \times 0.18 \times 0.25$	$0.22 \times 0.11 \times 0.36$	$0.12 \times 0.16 \times 0.22$
crystal colour	colourless	colourless	colourless
diffractometer	Enraf Nonius CAD4	Enraf Nonius CAD4	Enraf Nonius CAD4
data collection method	$\omega/2\theta$ scans	$\omega/2\theta$ scans	$\omega/2\theta$ scans
absorption correction	ψ scan	no correction	no correction
total data collected	8989	5735	5154
unique data	8676	5047	4655
observed data [$I > 2\sigma(I)$]	6375	4310	1135
R_{int}	0.0244	0.0527	0.0796
θ_{max} [°]	74.33	74.33	74.33
range of h, k, l	$-12 \le h \le 12$	$0 \le h \le 19$	$-18 \le h \le 0$
	$0 \le k \le 31$	$0 \le k \le 25$	$0 \le k \le 18$
	$-20 \le l \le 0$	$0 \le l \le 27$	$0 \le l \le 25$
no. of standard reflections	3	3	3
frequency of standard reflections [min]	120	120	120
intensity decay [%]	– 2.7	– 4.6	– 5.8
refinement on	F^2	F^2	F^2
R_1 [$F_o > 4\sigma(F_o)$]	0.050	0.072	0.127
wR_2 (F^2), all data	0.1575	0.2214	0.3850
S	0.88	1.15	0.85
parameters	991	827	218
largest difference peak hole [e Å^{-3}]	0.27 – 0.28	1.00 – 0.27	0.56 – 0.38
data reduction program	SDP[27]	HELENA[31]	HELENA
structure solution program	SIR92[28]	SHELXS97[32]	SHELXS97
struct. refinement program	SHELXL97[29]	SHELXL97	SHELXL97
preparation of material for publication (program)	PLATON98[30]	PLATON98	PLATON98

Hamley, A. B. Smith III, T. Beisine, K. Raynor, L. Maechler, C. Donaldson, W. Vale, R. M. Freidinger, R. Cascieri, C. D. Strader, *J. Am. Chem. Soc.* **1993**, *115*, 12550.

[7] a) C. D. Gutsche, *Aldrichimica Acta* **1995**, *28*, 3; b) P. Liunane, S. Shinkai, *Chem. Ind. London* **1994**, 811; c) V. Böhmer, *Angew. Chem.* **1995**, *107*, 785; *Angew. Chem. Int. Ed. Engl.* **1995**, *34*, 713.

[8] a) Transport and extraction of *Z*-amino acid carboxylates by rigid polycyclic calix[4]arene amino acid derivatives have been reported: Y. Okada, Y. Kasai, Y. Nishimura, *Tetrahedron Lett.* **1995**, *36*, 555; b) Lower rim amino acid derivatives: M. S. Peña, Y. Zhang, S. Thibodeaux, M. L. McLaughlin, A. M. de la Peña, I. M. Warner, *Tetrahedron Lett.* **1996**, *37*, 5841; c) Upper rim amino acid derivatives: T. Nagasaki, Y. Tajiri, S. Shinkai, *Recl. Trav. Chim. Pays-Bas* **1993**, *112*, 407.

[9] F. Sansone, S. Barboso, A. Casnati, M. Fabbi, A. Pochini, F. Ugozzoli, R. Ungaro, *Eur. J. Org. Chem.* **1998**, 897.

[10] D. M. Rudkevich, G. Hilmersson, J. Rebek, Jr., *J. Am. Chem. Soc.* **1997**, *119*, 9911.

[11] a) O. Mogek, V. Böhmer, W. Vogt, *Tetrahedron* **1996**, *52*, 8489; b) K. D. Shimizu, J. Rebek, Jr., *Proc. Natl. Acad. Sci. USA* **1995**, *92*, 12403.

[12] H. Murakami, S. Shinkai, *Tetrahedron Lett.* **1993**, *34*, 4237.

[13] Molecule **1** was built and its conformational space searched using SYBYL software of TRYPOS. Several low-energy conformations were identified that contained various numbers of NH$\cdots$O=C$\langle$ hydrogen bonds at the lower rim.

[14] a) S.-K. Chang, S.-K. Kwon, I. Cho, *Chem. Lett.* **1987**, 947; b) F. Arnaud-Neu, M.-J. Schwing-Weill, K. Ziat, S. Cremin, S. J. Harris, M. A. McKervey, *New J. Chem.* **1991**, *15*, 33; c) F. Arnaud-Neu, G. Barett, S. Fanni, D. Marrs, W. McGregor, M. A. McKervey, M.-J. Schwing-Weill, V. Vetrogon, S. Wechsler, *J. Chem. Soc. Perkin Trans. 2* **1995**, 453.

[15] *Synthese von Peptiden*, *Teil II*, *Band XV/2* (Eds.: J. Houben, T. Weyl), Thieme, Stuttgart, **1974**.

[16] a) M. A. McKervey, E. M. Seward, G. Ferguson, B. L. Ruhl, S. J. Harris, *J. Chem. Soc. Chem. Commun.* **1985**, 388; b) K. Iwamoto, S. Shinkai, *J. Org. Chem.* **1992**, *57*, 7066.

[17] R. Ostaszewski, T. W. Stevens, W. Verboom, D. N. Reinhoudt, M. Kasperse, *Recl. Trav. Chim. Pays-Bas* **1991**, *110*, 294.

[18] a) Y. Tor, J. Libman, A. Shanzer, C. E. Felder, S. Lifson, *J. Am. Chem. Soc.* **1992**, *114*, 6653; b) P. Guilbaud, A. Varnek, G. Wipf, *J. Am. Chem. Soc.* **1993**, *115*, 8298; c) E. S. Stevens, N. Sugawara, G. M. Bonora, C. Toniolo, *J. Am. Chem. Soc.* **1980**, *102*, 7048.

[19] A. Otter, X. Liu, G. Kotovych, *J. Magn. Reson.* **1990**, *86*, 657.

0947-6539/00/0603-0452 $ 17.50+.50/0 *Chem. Eur. J.* **2000**, *6*, No. 3

[20] a) V. Prelog, H. Gerlach, *Helv. Chim. Acta* **1964**, *47*, 2288; b) K. Mislow, *Chimia* **1986**, *40*, 17.
[21] F. Ugozzoli, G. Andreetti, *J. Inclusion Phenom. Mol. Recognit. Chem.* **1992**, *13*, 337.
[22] F. Arnaud-Neu, S. Fanni, L. Guerra, W. McGregor, K. Ziat, M.-J. Schwing-Weill, G. Barrett, M. A. McKervey, D. Marrs, E. Seward, *J. Chem. Soc. Perkin Trans. 2* **1995**, 113.
[23] F. Arnauld-Neu, G. Barett, S. Cremin, M. Deasy, G. Ferguson, S. J. Harris, A. J. Lough, L. Guerra, M. A. McKervey, M.-J. Schwing-Weill, P. Schwinte, *J. Chem. Soc. Perkin Trans. 2*, **1992**, 1119.
[24] C. J. Pedersen, *Fed. Proc.* **1968**, *27*, 1305.
[25] C. J. Thoman, *J. Am. Chem. Soc.* **1985**, *107*, 1437.
[26] J. D. Lamb, J. J. Christensen, R. M. Izatt, *J. Chem. Educ.* **1980**, *57*, 227.
[27] B. A. Frenz, SDP(VAX), Structure Determination Package, **1982**, College Station, Texas (USA).
[28] A. Altomare, M. C. Burla, M. Camalli, G. Cascarano, C. Giaccovazzo, A. Guagliardi, G. Polidori, *J. Appl. Crystallogr.* **1994**, *27*, 435.
[29] G. M. Sheldrick, *SHELX97*: *Program for the Refinement of Crystal Structures*, **1997**, Universität Göttingen (Germany).
[30] A. L. Spek, *PLATON98*: *A Multipurpose Crystallographic Tool*, *120398 Version*, **1998**, University of Utrecht, Utrecht (The Netherlands).
[31] A. L. Spek, *HELENA*, *Program for Data Reduction*, **1993**, University of Utrecht, Utrecht (The Netherlands).
[32] G. M. Sheldrick, *SHELXS-97*: *Program for the Solution of Crystal Structures*, **1997**, Universität Göttingen (Germany).

Received: April 19, 1999 [F1733]